Physica A 196 (1993) 519–545
North-Holland

SDI: 0378-4371(93)E0022-7

PHYSICA A

Monte Carlo simulations of a two-dimensional hard dimer system

K.W. Wojciechowski

Institute of Molecular Physics, Polish Academy of Sciences, Smoluchowskiego 17/19, 60-179 Poznań, Poland[1]
and International Centre for Theoretical Physics, Trieste, Italy

A.C. Brańka

Institute of Molecular Physics, Polish Academy of Sciences, Smoluchowskiego 17/19, 60-179 Poznań, Poland

D. Frenkel

F.O.M. Institute for Atomic and Molecular Physics, Kruislaan 407, 1098 SJ Amsterdam, The Netherlands

Received 26 October 1992

Monte Carlo simulations of a system of two-dimensional hard, homonuclear dimers are reported. The equation-of-state, structural and orientational properties, and the free energy were computed for the fluid phase and several crystalline and non-crystalline (non-periodic) solid structures. The differences in the Gibbs free energy between the various solid structures were found not to exceed $0.1k_BT$ per particle. This is much less than the contribution to the entropy per particle due to degeneracy of the 'ground state' of the non-periodic solid which amounts to $0.857k_BT$. Hence, the thermodynamically stable solid structure of the system corresponds to a set of non-periodic arrangements of the molecular centres of mass and orientations. The coexistence pressure of the non-periodic solid and fluid is determined; it is located within the observed narrow hysteresis region. It is shown that structures of the crystalline solids are well approximated by a simple lattice model.

1. Introduction

Many properties of real systems derive from purely geometrical effects. The best known example is the melting transition. Melting, which was observed in systems as simple as hard spheres in three dimensions [1–3] and hard discs in two dimensions [4,3] (2D), can be understood as a consequence of excluded

[1] Permanent address.

volume effects. The same effects are responsible for the existence of (at least certain) liquid crystals [5–12] and plastic crystals [13–16]. Studies of systems with purely geometrical interactions (hard body systems) in which the interaction energy is zero if no bodies overlap and infinite if any overlap occurs, clearly demonstrate that their properties depend essentially on the molecular shape. Knowledge of *how* the phase diagrams of such systems depend on the molecular shape is an important step in understanding the phase behaviours of real systems. Studies of various hard body systems broaden our experience in this field. At present, the only efficient method for quantitative studies of phase diagrams of hard body systems are computer simulations. In this paper we report Monte Carlo (MC) simulations of 2D hard homonuclear dimers, further referred to as *dimers*.

The dimer is a crude model for a diatomic molecule in two dimensions. It consists of two hard discs, 'atoms', of the same diameter σ and centres at a distance σ (σ will be our unit of length). Although the rather artificial nature of the dimers may be considered a disadvantage which is compounded by the pathological nature of 2D solids in general [17], the model has the advantage that it is conceptually simple and well suited for numerical simulation. Moreover, there exist systems in nature, for instance certain molecular layers adsorbed on crystalline surfaces, that can be considered as effective 2D systems of diatomics [18].

It is easy to see that the dimers can be arranged in such a way that the discs forming them form a triangular close packed lattice. Since such a structure is the densest packing of the discs [19], it is also the densest packing of the dimers. It is easy to see that there are many close packed structures of the dimers, and many of them are not periodic, see fig. 1. In fig. 2 three pairs of different clusters of the dimers, each pair of the same shape, are shown. Such clusters, amongst other, can be used to build various close packed structures of the dimers. Considering only the first pair of the clusters, it is easy to see that the entropy per dimer at close packing in the thermodynamic limit is *positive* and not less than $0.5 \ln 2 \approx 0.347$ (in k_B units). More detailed considerations [20] lead to better estimates of the degeneracy entropy [20b], the exact value of which is in fact much higher, namely $s_{deg} \approx \ln 2.356 \approx 0.857$. The positive degeneracy entropy competes at lower densities with the excluded volume effects (vibrational entropy). For random non-periodic structures, the kagomé lattice on which centres of mass of the dimers are distributed at close packing [21], can be distorted only locally at lower densities. On the other hand, generating a periodic structure allows for a global distortion of the kagomé lattice, which results in a higher vibrational entropy. It is not obvious a priori which of the effects will prevail and which structure will be stable below close packing. In particular it is not known what the solid structure is at melting.

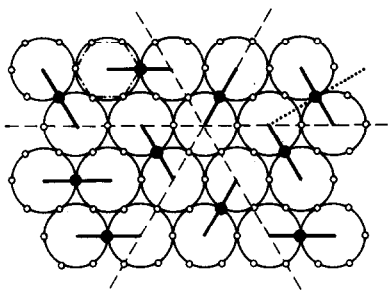

Fig. 1.

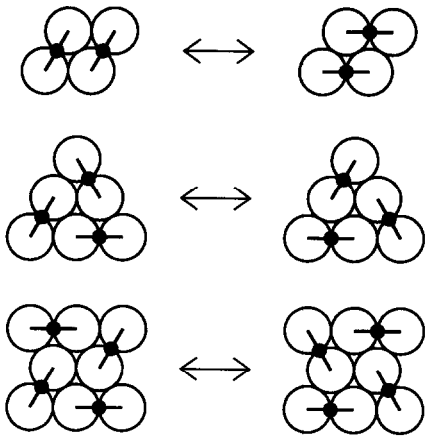

Fig. 2.

Fig. 1. Example of a non-periodic close packed lattice of the dimers. Black dots represent centres of mass of the dimers. Dashed lines indicate symmetry axes of the triangular lattice of disc-'atoms'. Small open circles mark sites of the kagomé lattice. The dash-dotted line is used to draw a unit hexagon of the kagomé lattice. It can be seen that positions of the dimer mass centres are restricted to the kagomé lattice sites; the decoration rule states that each unit hexagon (dash-dot line) contains exactly one centre of mass of a dimer. The dotted line indicates the 'short' dimer axis. The angle between the short axis and the x-axis of the laboratory frame defines the orientation of a dimer.

Fig. 2. Examples of equivalent clusters of the dimers. By replacing the corresponding clusters (indicated by double arrows) one can generate various arrangements of the dimers.

Mechanical simulations [22] and a theoretical study based on the free volume approximation [21] suggest that the degeneracy entropy prevails, and that in the solid state the molecular centres of mass and orientations of the dimers do not show any periodicity[#1]; this non-periodic phase will be further referred to as a disordered (or degenerate) crystal (DC).

The mechanical simulations and the free volume theory are only approximations, and the reliability of these approximations is not known a priori. To test the thermodynamic stability of the DC phase we performed computer simulations as these are, in principle, exact or, more precisely, they allow us to reduce the computational error to any desired level. As will be shown below, we do indeed find that the DC phase is stable. Hence, the dimer system is a simple example of a continuous homo-molecular model in which the molecules show no periodicity in the thermodynamically stable solid phase. As a by-product we compared the free energies of a few crystalline structures of the dimers and we analyzed structural properties of these crystals.

[#1] Obviously, at least at close packing, they show a certain long-range order as the dimer centres of mass are distributed on the kagomé lattice.

The structure of the paper is as follows: in the next section (2) a few close packed structures of the dimers are discussed which are studied in the following sections. In section 3, details of the MC simulations of the equation of state (EOS) and the structural properties of the dimer system are described. In section 4, results of these simulations are presented. For the solid structures, the isotherms, the unit cells parameters, and the orientational and radial distribution functions are analyzed. In the fluid phase, the discussion is limited to the EOS as the dimer fluid has been studied already by several other groups [23–25]. In particular, its structural properties were discussed in ref. [24]. In section 5, the free energy computations and the relative stability of the various solid structures studied is discussed, and the melting transition is located. The material presented in this section formed the basis for an earlier preliminary publication [26]. The last section (6) contains the summary and conclusions.

2. Dimer structures at close packing

In the thermodynamic limit there exist infinitely many close packed periodic structures of the dimers. In the present work we restricted ourselves to the four simplest. The number of molecules in the unit cell is used as the simplicity criterion: the fewer the number of molecules in the unit cell, the less information is necessary to describe the structure. It seems plausible that the simplest (in the above sense) periodic lattices should differ most, in thermodynamic and structural properties, from the non-periodic structures. The latter structures can be thought of as having infinitely many dimers in their 'unit cells'.

In fig. 3a–d the four periodic lattices studied in this work are shown. As is shown in appendix A, these lattices exhaust all the close packed periodic structures of dimers with no more than two molecules per unit cell. The structure A is a simple Bravais lattice (i.e., contains only one dimer in its unit cell) whereas the unit cells of the structures B, C and D consist of two dimers. The parameters of these structures at close packing are collected in table I.

Despite the existence of infinitely many regular lattices, the probability of a random choice of one of them from all the closely packed structures of the dimers is equal to zero. This is so, because the number of periodic structures is countable, whereas the number of all the structures is uncountable. Hence, any randomly chosen, closely packed structure of the dimers will be irregular, i.e., neither periodic nor self-similar. Studies of the DC phase require an algorithm allowing us to create the random lattices of the dimers. Such an algorithm was constructed using the cluster moves shown in fig. 2. The algorithm is based on two observations (discussed in detail in appendix B):

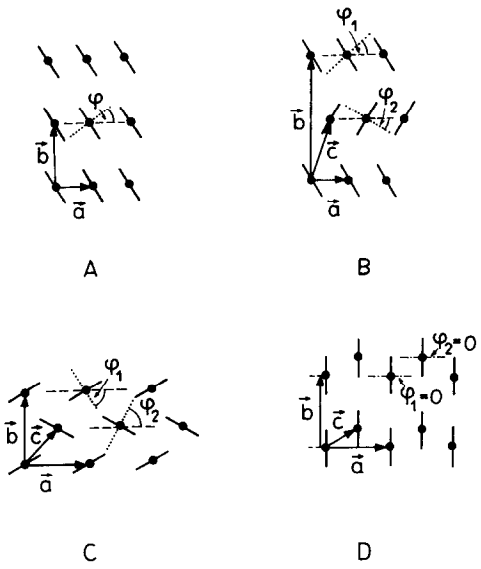

Fig. 3. Periodic structures of the dimers (only the dimer centres of mass and lines between centres of the disc-atoms are shown) with not more than two molecules per unit cell. Unit cell vectors and molecular orientations in the sublattices are indicated.

Table I
Structural parameters of the crystalline lattices with not more than two dimers per unit cell: $\boldsymbol{a}$, $\boldsymbol{b}$ are the unit cell vectors, $\boldsymbol{c}$ is the vector between the first and the second molecule of the basis, and ϕ_1, ϕ_2 are the angles between the x-axis and the 'short' molecular axes in the sublattices. $\boldsymbol{x}$ and $\boldsymbol{y}$ are the unit vectors of the x- and y-axes.

Lattice	A	B	C	D
$\boldsymbol{a}$	$\boldsymbol{x}$	$\boldsymbol{x}$	$\sqrt{3}\,\boldsymbol{x}$	$\sqrt{3}\,\boldsymbol{x}$
$\boldsymbol{b}$	$\sqrt{3}\,\boldsymbol{y}$	$2\sqrt{3}\,\boldsymbol{y}$	$2\boldsymbol{y}$	$2\boldsymbol{y}$
$\boldsymbol{c}$	–	$\frac{1}{2}\boldsymbol{x}+\sqrt{3}\,\boldsymbol{y}$	$\frac{1}{2}\sqrt{3}\,\boldsymbol{x}+\boldsymbol{y}$	$\frac{1}{2}\sqrt{3}\,\boldsymbol{x}+\frac{1}{2}\boldsymbol{y}$
ϕ_1	$\frac{1}{6}\pi$	$\frac{1}{6}\pi$	$-\frac{1}{3}\pi$	0
ϕ_2	–	$-\frac{1}{6}\pi$	$\frac{1}{3}\pi$	0

(1) No close packed structure of the dimers exists without any of the clusters shown in fig. 2,

(2) It is possible to transform *any* infinite close packed structure of the dimers into the periodic lattice A by applying the cluster moves; hence, these moves offer *ergodicity* at close packing.

Starting from any close packed lattice (e.g., a periodic one) and applying the cluster moves to randomly chosen molecules and their neighbours, one can transform the initial lattice into a (practically) random dense decoration of the kagomé lattice after a few trial moves per molecule.

3. Description of the MC simulations

We simulated $N = 112$ dimers by the MC method. For the solid phases most runs were performed in the NpT ensemble. Near melting a few runs were also done in the NVT ensemble. For the fluid phase both the ensembles were used on equal footing. Depending on the ensemble and the density of the system, the averages were taken over $(1–8) \times 10^4$ trial moves per particle (cycles) after an equilibration of $(0.5–2) \times 10^4$ cycles.

As for any hard body system, the EOS of the dimers relates the density, $\rho = N/V = v^{-1}$, to the ratio of the pressure and the temperature, p/T; N is the number of dimers and V the area of the system. We use dimensionless parameters $p^* = p\sigma^2/k_B T$ and $\rho^* = \rho/\rho_{cp} = v_{cp}/v = 1/v^*$, where k_B is the Boltzmann constant and ρ_{cp} is the density (the inverse of the area per particle, v_{cp}) at close packing.

The constant-pressure simulations of solids were started at high pressures, typically at $p^* = 30$. Initial structures were either the periodic lattices A, B, C and D or a certain non-periodic arrangement obtained by decorating the kagomé lattice (the initial relative area was chosen as $v^* = 1.05$). In subsequent runs the pressure was gradually reduced down to the point where the solid melted spontaneously. These 'melting' pressures differed slightly from one run to the next but they were never less than $p^* = 8.25$. A series of runs was also performed with increasing pressure, starting from a (defectless) DC structure into which the fluid froze spontaneously. (This was a *unique* case when the fluid froze into a *defectless* DC structure. Typically, the fluid froze into defect-rich DC structures, even if the pressure was increased very slowly.) In the simulations the shape of the periodic box was allowed to vary freely. This enabled the system to choose the equilibrium shape of the unit cell. To avoid rotation of the box one of its sides was kept parallel to the x-axis. The trial changes for the volume and shape were carried out approximately $N^{1/2}$ times more often than those of the individual particles. The particle moves consisted of simultaneous translations and rotations of the molecules. The maximal amplitude for the rotation (in radians) was twice as large as the amplitude for each component of the translation. The acceptance ratios for box moves and the particle moves were kept around 0.3–0.4. The standard particle moves did not lead to self-diffusion in the solid structures at the system size and run lengths used, i.e., the molecular arrangements were preserved, except at melting. We do not think that the lack of the self-diffusion is a serious obstacle for a proper sampling of the cystalline configurations. (The reason is that for stable crystalline structures the self-diffusion in most cases simply results in a relabeling of the particles.) In the case of non-periodic structures representing the DC phase, however, the self-diffusion usually leads to new molecular

arrangements. In order to sample various molecular arrangements of the DC phase we introduced transformations of certain particle groups (cluster moves) according to the idea presented in fig. 2. A sequence of N such trial moves was performed every 20 cycles. Technical details concerning these moves are described in appendix C. The typical acceptance ratios for the cluster moves were close to 0.03.

In the constant-area simulations of solids, the pressure was calculated by a direct generalization [27] of the method described in ref. [7]. In order to perform constant-area simulations of a solid that is free of stress, the shape of the simulation box must be chosen compatible with the equilibrium shape of the crystal unit cell. The latter shape was determined from analysis of the average box shape in constant -NpT simulations with a variable box shape. In the case of crystalline structures, the initial positions of the molecules were chosen as the lattice sites of a perfect lattice with the unit cell parameters determined from the constant-pressure data. The initial molecular orientations corresponded to maxima of the orientational probability density calculated from the NpT results. In the case of non-periodic structures, the random decorations of the kagomé lattice of the required density played the role of the initial configurations. The molecular moves and their acceptance ratios were similar to those in the NpT ensemble.

The fluid phase of the dimers was simulated in a square periodic box. The constant-pressure simulations were started at $p^* = 1.0$. In subsequent runs the pressure was increased up to spontaneous freezing of the system at $p^* = 8.75$. In the constant-area simulations the initial relative area was equal to $v^* = 1.27$. In subsequent runs this area was increased by uniform scaling, up to $v^* = 5.0$. As is easy to verify, a uniform and isotropic increase of the sample volume does not introduce overlaps to the system. (Dimers represent a particular case of the, so called, star-shaped bodies which are the most general case of shape with this property [27]. Such a property is, obviously, not true for non-convex bodies in general.) Other details of the simulations were similar to those for the solids, except that we did not use the cluster moves to compute the EOS data. In principle, one could use these moves also in the fluid. However, to satisfy the microscopic reversibility, this would require certain modifications of the program (either the operational definitions we used to identify clusters should be changed or some details in the execution of the cluster moves) which would result in slowing down the program rather than in improving the sampling. (A test sequence of a few runs in the fluid was performed, however, in which the cluster moves were restricted to the pair-clusters only. Starting from $p^* = 3$, the pressure was increased by $\Delta p^* = 1$ up to $p^* = 7$ in runs of 5×10^3 cycles, and then by $\Delta p^* = 0.5$ in runs of 10^4 cycles up to spontaneous freezing into the DC structure at $p^* = 9$. The results in the fluid EOS were the same as in the

standard runs, within the simulation error. The resulting DC structure contained two single-disc vacancies.)

4. The EOS and structural properties of the dimers

4.1. The EOS

The EOS data of the solid structures studied are collected in table II and plotted in fig. 4. As one can see, the isotherms are very close to each other. Within the accuracy of the present method, all the structures have the same

Table II
The solid branch of the EOS for $N = 112$ dimers. Typical runs in the NpT ensemble were 2×10^4 cycles (for the A lattice 10^4 cycles) after equilibration of 10^4 cycles. The relative areas superscripted by an asterisk correspond to runs of 4×10^4 cycles and those superscripted by two asterisks correspond to runs of 6×10^4 cycles. The error in $(v^* - 1)$ does not exceed 5 percent. In the NVT ensemble the runs were 4×10^4 cycles long and the estimated errors for $(p^* - 1/v^*)$ are about one percent.

p^*	v^* (NpT ensemble)				
	A	B	C	D	DC-phase
35	1.0487	–	–	–	–
30	1.0573	1.0584	1.0572	1.0595	1.0585*
25	1.0696	–	–	–	–
20	1.0881	1.0882	1.0878	1.0879	1.0876*
15	1.1175	1.1168	1.1171	1.1142	1.1197*
13.5	1.1317	1.1317*	1.1300	1.1306	1.1309*
12	1.1504	1.1471*	1.1484	1.1464	1.1500*
11	1.1607	1.1589*	1.1614	1.1639	1.1592*
10	1.1779	1.1756*	1.1804	1.1803	1.1812*
9.5	–	1.1864*	–	–	1.1912*
9	1.2044	1.1984*	1.2012	1.2021	1.2031**
8.75	–	1.2052**	–	–	1.2091**
8.5	1.2087	1.2145**	1.2122	1.2122	1.2166**
8.4	–	–	–	–	1.2185*
8.35	–	–	1.2161	1.2177	1.2210
8.25	1.2254	1.2199	–	–	–
v^*	p^* (NVT ensemble)				
1.18	–	9.84	–	–	–
1.2	–	–	9.07	–	9.11
1.22	–	8.26	–	–	–
1.23	–	8.02	8.02	–	8.07
1.24	–	7.77	–	–	–

isotherms, except near melting where the DC phase seems to be of slightly lower density than the remaining, periodic, structures.

In fig. 4 the EOS of the dimers is also compared with the EOS of hard discs [28]. The isotherm for hard discs is clearly above that for dimers. This can be understood by the following reasoning. In the solid phase of the hard disc system, the discs form a triangular lattice and each disc interacts (collides) practically only with its six nearest neighbours. The collisions lead to a certain effective interaction potential, u_{eff}, between the neighbouring discs, and the sum of the effective interactions over all pairs of neighbouring discs is simply the configurational free energy of the system. (Replacing the colliding discs by static points located on the average positions of the discs, i.e. on sites of a triangular lattice, and interacting with this effective potential, will, by definition, not change the EOS of the system. We stress, however, that such a replacement will change 'higher-order' properties of the system, e.g. elastic properties: in the hard disc system the ratio of the elastic moduli is approximately equal to three halves [29], whereas for the static lattice interacting via the effective potential this quantity is exactly equal to one.) Similar reasoning can be applied to the dimers in the DC phase, noting that the average positions of centres of the disc-atoms can be also approximated by sites of a triangular lattice (see section 4.4) and the interactions between the dimers can be 'decomposed' into interactions between the discs forming them. Thus, neglecting the degeneracy entropy term (which does not depend on the density), one can approximate the configurational free energy of the dimers by 5/6 of the configurational free energy of the hard disc system. (The factor 5/6 appears because each disc in the dimer system can collide with only five of its six nearest neighbours; the sixth neighbour belongs to the same dimer and its contribution to the interaction is zero.) The above approximate relation between the free energies of both the systems implies an approximate relation between their pressures:

$$p^*_{\mathrm{dimers}} = -\frac{\sigma^2}{k_{\mathrm{B}}T}\left(\frac{\partial(5U_{\mathrm{eff}}/6)}{\partial V}\right) = \tfrac{5}{6}p^*_{\mathrm{discs}}\,, \tag{1}$$

where $U_{\mathrm{eff}} = 3Nu_{\mathrm{eff}}(r)$ is the effective interaction energy of N hard discs arranged in a triangular lattice of the lattice side r. In fig. 4 the rescaled isotherm of the hard discs is also plotted. As one can see, the rescaled pressure for the hard disc system exceeds the pressure in the DC phase by only a few percent.

Some studies of the low-density ($v^* > 1.4$) dimer fluid have been reported in the literature [23–25]. Our results, obtained for the fluid phase both at lower densities as well as in the freezing region, are tabulated in table III and plotted

in fig. 5. In this figure the numerical data are also compared with the semi-empirical EOS proposed by Boublik [30]. This approximation was found to be most accurate amongst those considered in ref. [25]. As can be seen in fig. 5, this approximation overestimates the MC data at high densities. More recently the Percus–Yevick (PY) solution for the dimers, obtained at low

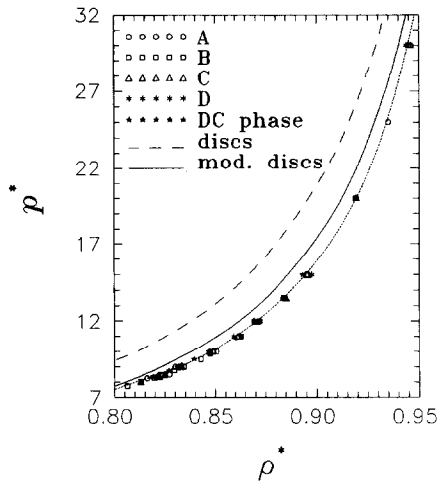

Fig. 4.

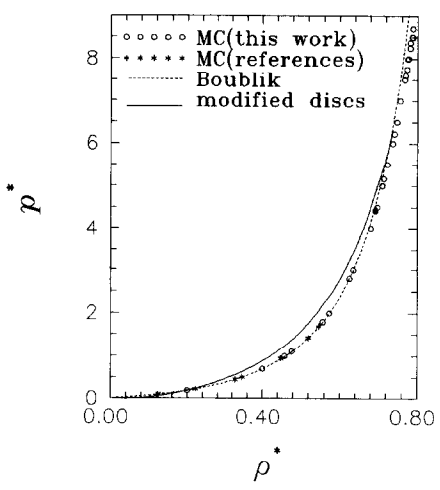

Fig. 5.

Fig. 4. Comparison of the EOS data for the solid structures studied with the EOS of hard disc (dashed line) and the EOS of hard discs rescaled by the factor $\frac{5}{6}$ (solid line).

Fig. 5. Comparison of the fluid branch of the dimer EOS with the equation proposed by Boublik [30] (dotted line) and the rescaled (see text) pressures of the hard disc system (the solid line).

Table III
The EOS data for the dimer fluid. Typical runs consisted of 2×10^4 cycles after 5×10^3 cycles equilibration. Asterisks in the *NpT* ensemble have the same meaning as in table II, whereas in the *NVT* ensemble they indicate runs of 8×10^4 steps. The initial run in the *NVT* ensemble was equilibriated during 2×10^4 cycles. The estimated errors are the same as in table II.

NpT				*NVT*			
p^*	v^*	p^*	v^*	v^*	p^*	v^*	p^*
1.0	2.184	6.5	1.338	1.27*	8.5	2.1	1.108
2.0	1.746	7.0	1.323	1.28*	8.37	2.5	0.699
3.0	1.575	7.5	1.304	1.29	7.99	5.0	0.1882
4.0	1.469	7.75*	1.294	1.3	7.6		
4.416*	1.443	8.0**	1.288	1.35	6.22		
4.5	1.433	8.25**	1.281	1.4	5.17		
5.0	1.406	8.5**	1.273	1.44338*	4.43		
5.5	1.382	8.7	1.270	1.6	2.798		
6.0	1.357			1.8	1.79		

densities [31], clearly underestimates the pressures. Hence, no theory is known as yet which accurately describes the dimer fluid over the whole density range.

In fig. 5 we draw for comparison the EOS for the hard disc fluid [31] with pressure rescaled by a density dependent factor, playing the same role as the factor 5/6 in the solid, obtained within the Kawamura theory of melting of the hard disc system [32]. It can be seen that the agreement with the dimer EOS is rather poor (in particular at low densities), what indicates that, contrary to the case of the solid, the 'atomic' structure of the dimer fluid is much different than the structure of the hard disc fluid.

4.2. *Unit cell parameters*

In table IV the parameters of the unit cells of the dimer crystals $a^* \equiv a/a_{cp}$, $b_x^* \equiv b_x/b_{cp}$ and $b_y^* \equiv b_y/b_{cp}$ are collected at different pressures. (b_x^* is tabulated only for the lattice A for which it is essentially different from zero; for the other structures b_x^* is equal to zero within the simulation error.) In fig. 6 the relative area dependences of these parameters are plotted for the studied structures. It follows from these plots that the unit cell parameters are smooth (almost linear) functions of the relative area. Approximating the MC data by smooth functions in v^* one can estimate their slopes at close packing. The slopes obtained from power fits are collected in the last row of table IV. The unit cell parameters of the studied periodic solids are compared in fig. 6 with two simple models:

(i) a *hard static model* in which the structure is calculated for an n-inverse-power interaction between the centres of the discs forming dimers and then the limit $n \to \infty$ is taken;

(ii) a *soft static model* in which the dimers interact by a *site–site* effective potential:

$$u(r) = -\tfrac{2}{3} k_B T \ln(r/\sigma - 1) ,$$

and it is assumed that only the discs being the nearest neighbours (which have a common side of their Dirichlet polygons) interact with each other.

The latter potential, obtained for the hard disc system in the self-consistent free volume approximation [33,34], is a simple but quite accurate approximation of the effective interaction potential mentioned in the previous subsection.

We observe that the differences between these models and the numerical data do not exceed a few percent in the case of the unit cell sides. This can be considered good agreement if we take into account the non-analytic character of the dimer interaction and simplicity of the models.

Table IV
The relative area dependence of the unit cell sides in the periodic structures. The estimated slopes of a^* versus the relative area at close packing are presented in the last row.

p^*	A			B		C		D	
	a^*	$10^2 b_x^*$	b_y^*	a^*	b_y^*	a^*	b_y^*	a^*	b_y^*
35	1.0296	1.85	1.0185	–	–	–	–	–	–
30	1.0354	2.12	1.0212	1.0363	1.0213	1.0224	1.0341	1.0452	1.0136
25	1.0427	2.68	1.0259	–	–	–	–	–	–
20	1.0552	3.27	1.0313	1.0537	1.0418	1.0339	1.0522	1.0665	1.0201
15	1.0710	4.50	1.0434	1.0720	1.0467	1.0440	1.0700	1.0863	1.0257
13.5	1.0806	4.82	1.0472	1.0811	1.0529	1.0489	1.0773	1.0989	1.0289
12	1.0941	5.78	1.0515	1.0895	1.0549	1.0556	1.0880	1.1107	1.0322
11	1.0998	5.69	1.0554	1.0986	1.0586	1.0582	1.0975	1.1244	1.0352
10	1.1096	6.64	1.0615	1.1095	1.0675	1.0681	1.1051	1.1360	1.0389
9.5	–	–	–	1.1113	1.0685	–	–	–	–
9	1.1292	7.92	1.0667	1.1216	1.0694	1.0726	1.1199	1.1543	1.0415
8.75	–	–	–	1.1270	1.0694	–	–	–	–
8.5	1.1259	8.58	1.0735	1.1319	1.0730	1.0738	1.1289	1.1626	1.0427
8.4	–	–	–	–	–	–	–	–	–
8.35	–	–	–	–	–	1.0772	1.1289	1.1657	1.0446
8.25	1.1377	9.06	1.0771	1.1335	1.0763	–	–	–	–
Slope	0.635	0.38	0.365	0.633	0.367	0.384	0.616	0.775	0.225

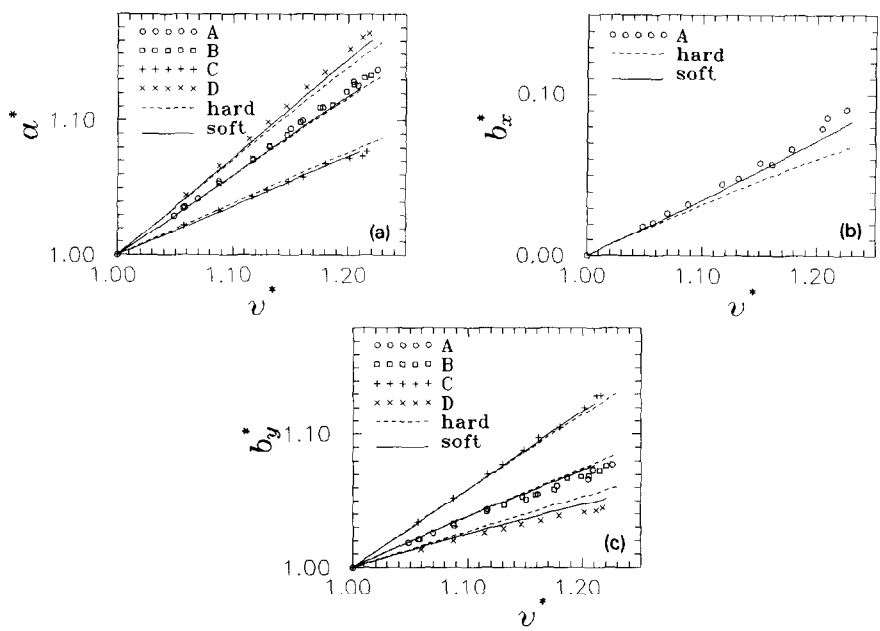

Fig. 6. The MC results for the relative area dependence of the unit cell vectors of the periodic structures studied compared with the lattice models described in text: (a) a^*, (b) b_x^* and (c) b_y^*. In case (b), the comparison is shown only for the structure A (which exhibits essentially non-zero value of the x-component of the unit cell vector $\boldsymbol{b}$).

The second of the models defined above can also be used to calculate the isoterms of the solids. (The first model gives, obviously, zero pressure below the close packing.) The agreement between the calculated EOS and the MC data is, however, worse than in the case of the structural data.

More detailed characteristics of the non-Bravais structures B, C and D requires also specification of the basis vector, $\boldsymbol{c}$. For the structures B and C, within the simulation accuracy, the basis vectors were found to be equal to one half of the sum of the unit cell vectors, $\boldsymbol{c} = (\boldsymbol{a} + \boldsymbol{b})/2$. In the case of the structure D, this relation holds only for the x-component of the vector $\boldsymbol{c}$. The y-component of this vector was equal to $\sigma/2$, i.e. the same as at the close packing.

For the DC phase the relative box sides $a^* \equiv u_x/u_{x0}$ and $b^* \equiv v_y/v_{y0}$ play the same role as the relative unit cell sides for periodic structures; u_x and v_y are the components of the box sides $\boldsymbol{u}$ and $\boldsymbol{v}$, and u_{x0} and v_{y0} are their values at close packing. Within the accuracy of the simulations, the quantities a^* and b^* were equal to each other down to melting, i.e. the system preserved its initial shape, corresponding to a random decoration of the kagomé lattice.

Closing this section, we would like to stress that the above structural data are expected to characterize only the *local* order in the system. This comes from the well known fact that the long-range translational order is absent in 2D (strictly speaking, the formal proof did not concern hard potentials [17] but simulations of the hard disc system by Alder and Young demonstrated this in a convincing way [35]).

4.3. Molecular orientations

For analysis of the molecular orientational order in the system we computed the orientational probability distribution. Examples of such distributions for the solid structures studied are shown in fig. 7. It can be seen there that these

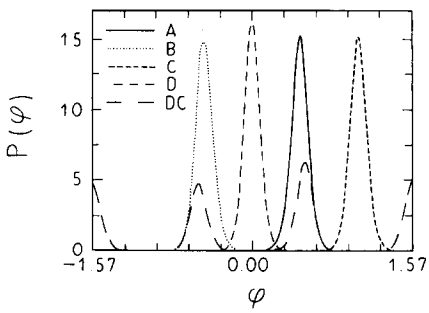

Fig. 7. Typical orientational probability density distributions (normalized to π) in the solid phases of the dimers at $p^* = 12$. For the lattices B and C the curves are drawn for the second sublattice only (see fig. 3).

Table V
Mean orientations of dimers and variances of the dimer orientations in solids.

p^*	A		B		C		D		DC
	$\langle\phi\rangle$	$\langle(\phi-\langle\phi\rangle)^2\rangle$	$\langle\phi\rangle$	$\langle(\phi-\langle\phi\rangle)^2\rangle$	$\langle\phi\rangle$	$\langle(\phi-\langle\phi\rangle)^2\rangle$	$10^3\langle\phi\rangle$	$\langle(\phi-\langle\phi\rangle)^2\rangle$	$\langle(\phi-\langle\phi\rangle)^2\rangle$
35	0.506	2.71×10^{-3}	–	–	–	–	–	–	–
30	0.504	3.16×10^{-3}	0.504	3.18×10^{-3}	1.047	3.16×10^{-3}	2.3	3.30×10^{-3}	3.27×10^{-3}
25	0.499	3.92×10^{-3}	–	–	–	–	–	–	–
20	0.494	5.01×10^{-3}	0.493	4.86×10^{-3}	1.049	4.96×10^{-3}	3.4	4.92×10^{-3}	4.93×10^{-3}
15	0.480	6.73×10^{-3}	0.484	6.50×10^{-3}	1.050	6.71×10^{-3}	4.8	6.39×10^{-3}	6.84×10^{-3}
13.5	0.477	7.62×10^{-3}	0.478	7.66×10^{-3}	1.051	7.54×10^{-3}	4.9	7.40×10^{-3}	7.55×10^{-3}
12	0.471	9.00×10^{-3}	0.471	8.54×10^{-3}	1.051	8.78×10^{-3}	5.4	8.34×10^{-3}	8.83×10^{-3}
11	0.469	9.45×10^{-3}	0.469	9.44×10^{-3}	1.050	9.57×10^{-3}	9.0	9.52×10^{-3}	9.37×10^{-3}
10	0.460	1.09×10^{-2}	0.463	1.04×10^{-2}	1.055	1.09×10^{-2}	6.9	1.07×10^{-2}	1.10×10^{-2}
9.5	–	–	0.452	1.13×10^{-2}	–	–	–	–	1.18×10^{-2}
9	0.452	1.31×10^{-2}	0.451	1.22×10^{-2}	1.051	1.24×10^{-2}	6.5	1.25×10^{-2}	1.26×10^{-2}
8.75	–	–	0.449	1.27×10^{-2}	–	–	–	–	1.32×10^{-2}
8.5	0.439	1.35×10^{-2}	0.443	1.32×10^{-2}	1.048	1.36×10^{-2}	6.9	1.31×10^{-2}	1.38×10^{-2}
8.4	–	–	–	–	–	–	–	–	1.40×10^{-2}
8.35	–	–	–	–	1.051	1.37×10^{-2}	5.7	1.36×10^{-2}	1.42×10^{-2}
8.25	0.433	1.54×10^{-2}	0.438	1.36×10^{-2}	–	–	–	–	–

distributions are concentrated around certain values of the angles. We characterized these distributions by computing the mean molecular angle and its variance. The mean molecular orientations for the periodic solids (calculated on intervals of lengths π and centred on angles of maximal probability density) are collected in table V. A comparison of the mean orientations for the structures A and B (in the latter case a single sublattice is considered) with the lattice models described in section 4.2 is shown in fig. 8. As one can see, in the case of the molecular orientations the second model is much closer to the MC data. The same holds true for the other structures studied. For the DC phase

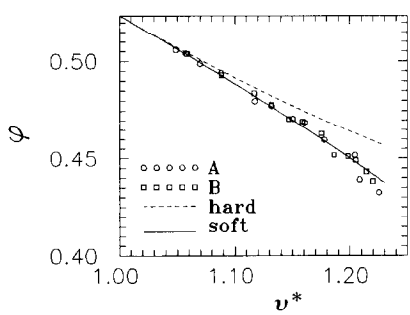

Fig. 8.

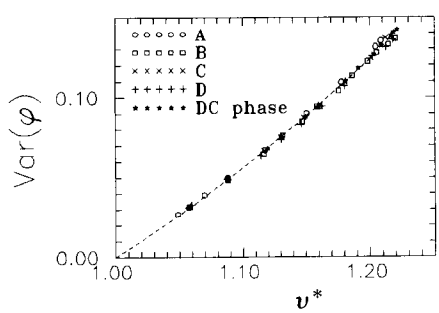

Fig. 9.

Fig. 8. The MC results for the relative area dependence of the mean angle (between the short molecular axes and the x-axis) in the structure A and in the first sublattice of the structure B compared with the lattice models described in the text.

Fig. 9. Relative area dependence of the variances of the dimer orientations in the studied solids. For the lattices B and C these quantities correspond to a single (averaged) sublattice. In the case of the DC phase a single (averaged) maximum is analyzed.

the orientational distributions consisted of three distinct peaks centred at $\pm\pi/6$ and $\pi/2 (\equiv -\pi/2)$. The average molecular orientation in this phase, calculated in the interval $(-\pi/2, \pi/2)$, was equal to zero, within the experimental error.

The amplitude of librational moves of the dimers in the solid structures can be characterized by the width of the maxima of the orientational distribution function. The obtained orientational mean square displacements of the dimers are collected in table V and plotted versus the relative area in fig. 9. The plot indicates that the orientational 'freedom' of the dimers is almost the same in all the solid structures studied, and it is a smooth function of v^*. Using polynomial fits in v^* one can estimate its slope at $v^* = 1$. For the solid structures studied, this quantity is found to be bracketed by 0.5 from the below and by 0.53 from the above.

4.4. *Radial distribution functions (rdf's)*

Atom–atom (AA) and molecular-centre–molecular-centre (CC) radial distribution functions (rdf's) were computed at a few densities. In figs. 10a, b the AA rdf of the DC phase of dimers is compared with the rdf of hard discs at the same relative area. It can be seen that the positions of the first maxima of these functions in both the systems are nearly the same. This observation supports the concept of the average triangular lattice of hard disc-atoms used in the discussion of the dimer EOS (section 4.1).

In fig. 10c the CC rdf of the DC phase is drawn. The positions of the maxima of this function are compared with the positions corresponding to random decorations of the kagomé lattice by dimers at the same density. As one can see, the actual rdf profiles can be thought of as obtained by smearing the distributions corresponding to the perfect kagomé lattice. This indicates that the structure of the DC phase can be seen as a random decoration of the kagomé lattice by the dimer centres of mass. This picture, complementary to the picture in which the structure of the DC phase is treated as a triangular lattice of discs-atoms, will be further exploited in the construction of the reference configurations for free energy calculations.

5. Free energy computations and location of the melting transition

The NpT simulations of the dimer EOS suggest that the melting phase transition in this system occurs at certain pressure, p_{melting}, which is bracketed by 8.25 from the below and 8.75 from the above. It does not follow, however, from the EOS data what is the structure of the thermodynamically stable dimer solid. As mentioned in the introduction, one should distinguish at least two possibilities:

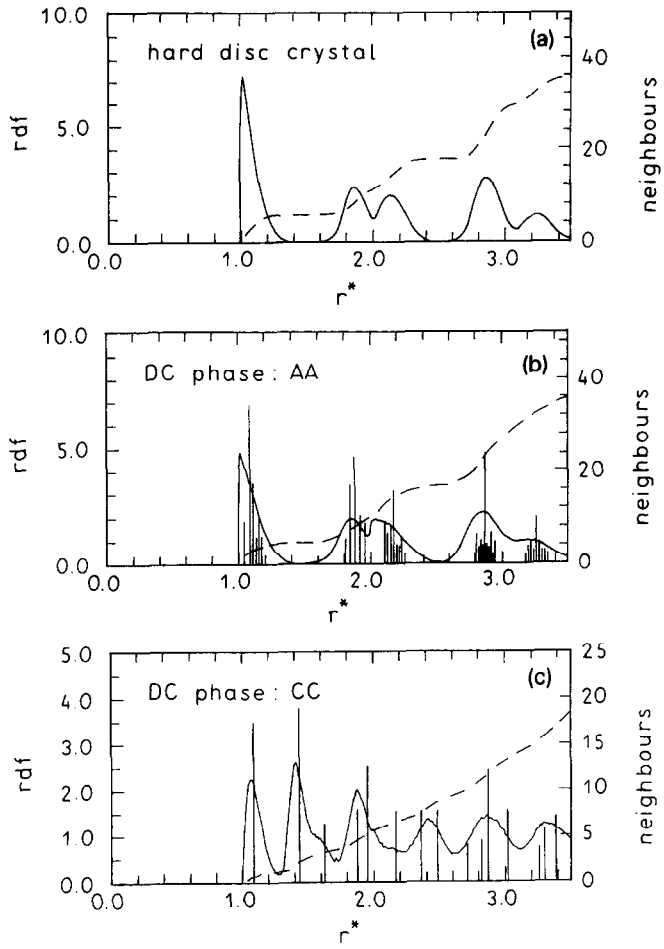

Fig. 10. Radial distribution functions (solid lines) and accumulation plots (dashed lines) at $v^* = 1.18$: (a) hard disc crystal, (b) AA-function for dimers and (c) CC-function for dimers. In (b) and (c) the positions of the maxima of the corresponding rdf's for the kagomé lattice decorations are shown. The latter maxima correspond to a single non-periodic decoration of the kagomé lattice and, hence, their amplitudes do not necessarily correspond to those of the DC phase.

(i) the thermodynamically stable phase corresponds to a periodic arrangement of the dimers,

(ii) the thermodynamically stable phase corresponds to many molecular arrangements, constituting the DC phase.

It is worth noting that from a purely formal point of view it is also possible that a certain single *non-periodic*, e.g. self-similar, structure can be the stable one. Such a possibility seems to be, however, very unplausible in the case of the dimers because global distortions of the kagomé lattice (offered by simple

periodic structures) should increase the vibrational entropy of the dimers more than local ones (offered by self-similar structures).

Which of the possibilities applies can be decided by comparing free energies of various solid structures. Below we describe calculations of the free energies per particle (further on, the Helmholtz/Gibbs free energy and the entropy are calculated *per particle*) performed for each of the studied solid structures and the fluid. Knowledge of the free energy of the latter phase allows for independent location of the melting transition.

5.1. *Free energies of solids and thermodynamic stability of the DC phase*

The free energies of the solid structures were calculated using the Einstein crystal (EC) method [36,8]. The details of the calculations were similar to those described in ref. [37]. The computations for all the studied solids were performed at $v^* = 1.18$, i.e. at a point inside the (mechanical) stability region of all the solid phases considered. For the periodic structures the reference EC configurations were chosen as perfect crystals of unit cell parameters and molecular orientations determined by analysis of the NpT averages. The reference configurations for the DC phase were represented by seven randomly generated decorations of the kagomé lattice. The average value of the free energies of these structures was considered as the free energy of a typical, single, DC structure. The free energies obtained for the solid structures are tabulated in table VI; the notation is the same as in the ref. [37]. It can be seen there that the free energies of the periodic solids, being very close to each other, are lower than that of the typical non-periodic structure. Amongst the periodic crystals the lattices A, B and C have practically the same free energies, whereas the lattice D is slightly less stable compared to the former three. This is what one may expect on basis of an analysis of a slightly more general system. Namely, one can consider analogues of the periodic lattices A, B, C and D in the case that the molecules are not dimers but dumbbells (the discs forming the dumbbell not only touch each other, as in the case of the

Table VI
The free energies, f, of the dimer solids at $v^* = 1.18$ (t.s. means typical structure); notation is the same as in ref. [37].

Structure	$\lambda_{tr}^{max} = \lambda_{rot}^{max}$	Integral	f_{corr}	$f_{EC}^{c.m.} - N^{-1} \ln(Nv^* v_{cp})$	f_{solid}
A	1000	3.777(16)	0.0048(3)	8.5867	4.815(16)
B	1000	3.775(12)	0.0047(3)	8.5867	4.816(12)
	40000	9.25(4)	0.0000	14.0873	4.83(4)
C	1000	3.772(16)	0.0051(4)	8.5867	4.820(16)
D	1000	3.732(17)	0.0037(2)	8.5867	4.859(17)
$DC_{t.s.}$	1000	3.723(18)	0.048(4)	8.5867	4.912(22)

dimers, but overlap slightly, i.e. the distance, $d = d^*\sigma$, between centres of the discs forming the dumbbell is less than σ). It is easy to verify that the structures A, B, C have their stable dumbbell analogues. The area per dumbbell at close packing is in these cases the same and equal to

$$v_{cp}^{A}(d^*) = [\sqrt{3}/2 + d^*(1 - d^{*2}/4)^{1/2}]\sigma^2 .$$

On the other hand, the direct (rectangular-lattice) analogue of the structure D has lower density at close packing because

$$v_{cp}^{D}(d^*) = (1 + d^*)(1 - d^{*2}/4)^{1/2}\sigma^2 > v_{cp}^{A}(d^*) .$$

Moreover, the rectangular D structure of the dumbbells is not stable and to make it stable a rearrangement of the dumbbells is necessary. Even after this rearrangement, the D structure is not as dense as the remaining three structures. It is natural to expect that also at lower densities in the dumbbell system the structure D will correspond to a higher free energy than the remaining three structures. The above discussion suggests that the D structure of the dimers cannot be more stable than the other three periodic structures studied. This is so, because the anisotropy parameter d^* can be used as a parameter of the free energy and one can go to the limit $d^* \to 1$ (continuity of the free energy as a function of d^* is assumed). The case in which (below the close packing) the free energies $f_D(d^*) > f_A(d^*)$ tend to the same limit is intuitively not plausible (although possible, in general) and hence one expects that the D phase in the dimer system is less stable than the other three periodic ones.

The computed free energies and the EOS results were used to estimate the Gibbs free energies, $g = f + pv$, of the considered structures in the hysteresis region. The obtained values are collected in table VII. It can be seen there that the differences between the Gibbs free energies per particle for very different solid structures do not exceed 0.1 (in $k_B T$ units). This is much less than the contribution coming from the degeneracy entropy which amounts to -0.857 (in the same units) to the Gibbs free energy per particle. Such a situation makes impossible that any *single* (periodic or not) solid structure of the dimers could

Table VII
The Gibbs free energies, g, of the studied phases in the hysteresis region (t.s. means typical structure). The errors are about 10 percent larger than those in table VI.

p^*	g_A	g_B	g_C	g_D	$g_{DC}^{(t.s.)}$	g_{fluid}	g_{DC}
8.35	21.830	21.836	21.836	21.874	21.922	21.035	21.064
8.7	22.565	22.571	22.571	22.610	22.658	21.807	21.801

be a thermodynamically stable phase close to melting. Hence, we conclude that the DC phase, which does not correspond to any single crystalline structure (as it is a rule for atomic crystals) but consists of infinitely *many* different macroscopically equivalent structures, is thermodynamically stable near melting.

The difference between the relative area of the DC phase and other studied solids can be roughly bounded by $\Delta v < 0.02\sigma^2$. The Gibbs free energy difference between the DC phase and any of the crystals considered can be written as

$$h_{\mathrm{DC}} - h_{\mathrm{crystals}} = \Delta h < \Delta h_{\mathrm{melting}} + (p - p_{\mathrm{melting}})\,\Delta v\,. \tag{2}$$

Elementary calculations, with $\Delta h_{\mathrm{melting}} \approx -0.7$ (see table VII) and $8.25 < p_{\mathrm{melting}} < 8.75$, show that this difference is negative, i.e. the DC phase is more stable than the other structures, in the whole range of the pressures studied.

Assuming that the entropy difference between the DC phase and any periodic crystal is a continuous function of the relative area for $v^* \geq 1$, one immediately gets that the DC phase is also the stable one near close packing. This is the consequence of the positive degeneracy entropy per particle of the DC phase – and zero entropy of the crystal there (both the DC phase and the periodic solid have the same close packing limit). Analysis of the free energy differences of the static models with the site–site effective interaction potential $-\frac{2}{3}k_{\mathrm{B}}T\ln(r/\sigma - 1)$, used in section 4, also indicates that the DC phase should be the stable one near the close packing (see appendix D). Thus, we expect that the DC phase is stable in the whole range of the densities above melting.

5.2. *Free energy of the fluid and location of the melting transition*

The MC pressures obtained for the fluid branch were fitted by the six-order density expansion

$$p = p_{\mathrm{id}} + B_2\rho^2 + B_3\rho^3 + \sum_{k=4}^{6} B_k\rho^k\,, \tag{3}$$

with the exact value of the second virial coefficient $B_2 = \frac{5}{6}\pi + 1/\pi + \frac{1}{2}\sqrt{3}$ [38] and $B_3 = 0.749B_2^2$ [24]. The above polynomial fit was then integrated analytically to determine the free energy according to the formula

$$f_{\mathrm{fluid}} = f_{\mathrm{id}} + \int_0^{\rho} (p - p_{\mathrm{id}})\rho^{-2}\,\mathrm{d}\rho\,, \tag{4}$$

where $f_{id}/k_BT = -\ln(\pi v) - 1$ is the free energy of non-interacting dimers (ideal gas).

Knowing the free energy of the fluid one can calculate its Gibbs free energy. Values of the Gibbs free energy of the fluid in the hysteresis region around melting are shown in table VII. As it is easy to note, the Gibbs free energy of the fluid at freezing is much lower than the Gibbs free energy of any individual solid structure (of the studied ones) at the same pressure, no matter whether the structure is periodic or not. The DC phase contains, however, the additional degeneracy entropy (per particle), $s_{deg} \approx 0.857 k_B$. Taking this entropy into account we locate the melting transition at $p^*_{melting} = 8.6(2)$, i.e. in the observed hysteresis region. The estimated melting density of the DC phase is $\rho^*_{DC} = 0.824(3)$ whereas the freezing density of the fluid is $\rho^*_{fluid} = 0.787(4)$.

6. Summary and conclusions

The equation of state and structural properties of the system of hard dimers were studied by the MC simulations. The simulations showed that the isotherm of the system consists of two branches: a fluid and a solid one. The branches are disjoint by a first order melting transition. In the fluid, the MC data were compared with some known approximate theoretical results for the EOS. This comparison showed that although none of the known theoretical approximations accurately reproduces the experimental results in the entire density range of stability of the fluid, the recent semi-empirical EOS proposed by Boublik [30] fails only near freezing. In the solid, the structural properties of crystalline (metastable) phases were found to be reasonably reproduced by simple lattice models considered in section 4. These models appeared, however, to be too simple for quantitative description of the EOS in the solid.

The free energy computations of various solid phases of the dimers showed that the DC phase is stable at melting and in the entire density range studied in our simulations. In section 5 we argued that the DC phase, which corresponds to infinitely many various, macroscopically equivalent, arrangements of the dimers, should be also thermodynamically stable near close packing. Hence, as there is no physical reason to assume a re-entrant behaviour in this system, we expect that the DC phase is the only thermodynamically stable solid phase of the dimers. Comparison of free energies of a few crystalline structures of the dimers showed that, as one could expect, the individual non-periodic structures are less stable than the periodic ones. Amongst the latter, the most stable appear those which have the densest analogue in dumbbell systems.

We close this paper with the following remarks:

(1) The cluster moves introduced in this paper can be considered as ergodic

at close packing. For this reason they may find applications in studies of various models which refer to decorations of the triangular lattice by dimers.

(2) The DC structure is stabilized by the degeneracy entropy. In this aspect it is similar to the so-called entropic quasicrystals [39]. At close packing, the DC phase exhibits also other essential properties of the quasicrystals: (i) there is only a finite number of possible bonds between the mass centres of neighbouring dimers, (ii) each such a bond has a finite number of possible orientations (6 or 12) and (iii) there is only a finite number of the unit cells (≡ surroundings of a chosen dimer). It should be stressed, however, that at close packing the DC phase exhibits an essential difference with respect to quasicrystals: all the possible positions of the dimer centres of mass in the DC phase are restricted to sites of the kagomé lattice, which is a *periodic* lattice, whereas, by definition, no periodic lattice of positive lattice constants exists which would contain sites of a quasiperiodic lattice. Hence, at least at close packing, the DC phase *is not* a quasicrystal. To stress the role of the degeneracy entropy and the existence of the 'supporting' periodic lattice, one could call this phase *entropic* '*crystal*' where the quotation marks are used to stress the lack of the truly long-range translational order in the system below the close packing.

(3) From a point of view of single disc-atoms forming the dimers, the DC phase can be seen (in average) as a triangular lattice. Thus, despite the presence of the intra-molecular bondings, in a large time-scale the dimer system can be seen as an 'atomic' solid. This suggests that the degeneracy entropy may be important also in certain real atomic crystals obtained by compressing molecular crystals under very high pressures [40].

Acknowledgements

The work of the Institute of Molecular Physics of the Polish Academy of Sciences was supported by the Polish Committee for Scientific Research (Grant No. 209789101). The work of FOM is a part of the research program of FOM and was supported by the Netherlands Organization for Scientific Research (NWO). One of us (K.W.W.) would like to thank Professor M.P. Tosi for his help and encouragement at the beginning of this project, and Dr. Piotr Pierański for useful conversations. He is also grateful to Professor Abdus Salam, the International Atomic Energy Agency, and UNESCO for hospitality at the International Centre for Theoretical Physics (I.C.T.P.) in Trieste where the manuscript was completed during the Research Workshop in Condensed Matter, Atomic and Molecular Physics.

Appendix A. Close packed periodic structures of the dimers with one or two molecules per unit cell

Analysis of fig. 11 proves that only one close packed lattice of dimers with a single molecule per unit cell exists. This lattice, further referred to as A, is shown in fig. 3a.

There exist only three closely packed lattices with two dimers per unit cell. This can be proven by considering translations of all essentially different (non-isometric) clusters of neighbouring dimers on the triangular lattice. (It is obvious that at least one of the atoms neighbouring to a chosen dimer cannot belong to the periodic image of the dimer; otherwise the unit cell contains only one molecule.) As is easy to check, there are only six such clusters. They are shown in fig. 12. These clusters can be used as bases generating all the possible lattices with one or two molecules per unit cell. Analysis of possible occupations of the lattice sites, marked by crosses in fig. 12, by translational images of these clusters leads to the following conclusions: (i) the cluster 5 does not generate any lattice (the crossed site cannot be the translational image of any of the cluster sites without creating overlaps with other sites of the cluster), (ii) the clusters 1 and 4 generate the lattice A, (iii) the clusters 2 and 3 generate

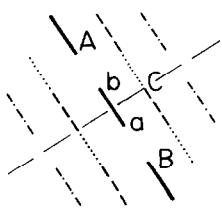

Fig. 11.

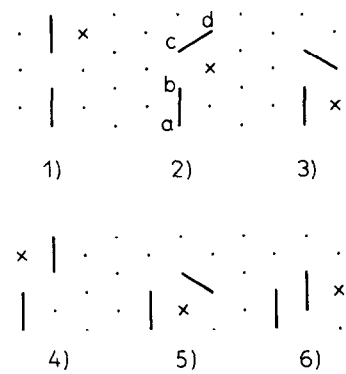

Fig. 12.

Fig. 11. The dimer (represented by a solid line) consisting of 'atoms' a and b is any dimer of any close packed, periodic lattice with one molecule per unit cell. It is obvious that the site A, neighbouring to b within the line ab, must be occupied by the image of the atom a, whereas the site B, neighbouring to a within the line ab, must be occupied by the image of the atom b. By induction, positions of all the dimers on the straight line ab are uniquely determined. (These dimers are also represented by solid lines.) The site C, being the nearest neighbour of the sites a and b, can be occupied either by the image of a or by the image of b. The first choice leads to the lattice A (see table I) whereas the second choice leads to its mirror image with respect to the bisectrix of the interval ab.

Fig. 12. Essentially different clusters formed by two neighbouring dimers.

the lattices B and C, see fig. 3b, c, respectively and (iv) the cluster 6 can generate either the lattice A or the lattice D shown in fig. 3d.

Appendix B. Ergodicity of the dimer system in presence of the cluster moves

Below we show that the cluster moves shown in fig. 2 allow for representative sampling of the DC phase even at close packing.

Let us note first that it is impossible to construct a close packed lattice without at least one of the clusters shown in fig. 2. The idea of the proof is illustrated in fig. 13. (To be precise, one could restrict considerations to pairs and quadruplets only. Triplets were introduced to simplify the proofs.)

Applying the cluster moves to any infinite close packed structure, one can transform it into the periodic lattice A. This can be shown in four steps:

(1) starting from the initial structure one constructs in it an infinite row of neighbouring molecules whose 'long' axes are parallel to the straight line containing their centres,

(2) near the constructed row one constructs a stripe of an arbitrary number of such rows,

(3) the constructed finite-width stripe of parallel dimers is then transformed into either a (parallel to the 'long' molecular axes) stripe of the perfect lattice A (or its symmetric image) or such a stripe with one stacking fault (as shown in fig. 14); when the number of the rows is odd the stacking fault can be always removed,

(4) in the thermodynamic limit (infinite width of the stripe) the stacking fault can be moved to infinity, and one obtains the lattice A.

The above steps are elementary but tedious (they require considering a large number of possible cases) and we avoid presenting them here.

For a finite system of dimers in a periodic box the close packed dimer structures can be divided into distinct sets of structures which correspond either

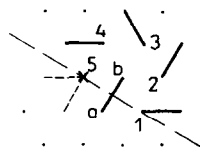

Fig. 13. The dimer occupying the lattice sites marked by a, b is any dimer of any close packed structure of dimers. If one wants to avoid the presence of the clusters shown in fig. 2 in this structure, there are only two symmetric (with respect to the broken line) ways of putting another dimer into the site 1. If one of these possibilities is chosen (e.g., that marked by a solid line) then three other sites (marked here by 2, 3, and 4) can be decorated in a single way. It is easy to see that by decorating the site 5 one cannot avoid creating a pair-cluster with one of the already placed dimers.

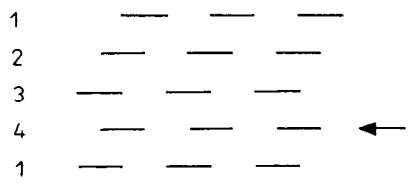

Fig. 14.

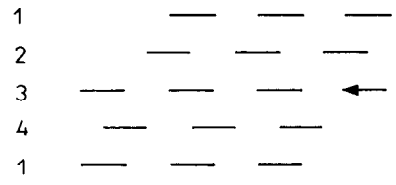

Fig. 15.

Fig. 14. The lattice A with a stacking fault indicated by the arrow.

Fig. 15. The lattice A (with periodic boundary conditions) with a shifted row indicated by the arrow.

to the perfect lattice A or to such a lattice with a stacking fault or a shifted row, see fig. 15. Some test runs we performed did not show any differences of structural and thermodynamic properties between the DC configurations representing these sets.

Appendix C. Cluster moves

The trial cluster moves were performed in sequences consisting of individual N moves. Each individual move can be divided into four parts:

(1) One of the dimers is randomly chosen. (The same dimer can be chosen a few times in a single sequence of N moves.)

(2) The kind of cluster to be tried to move is randomly selected. (In the present work each of the three kinds of clusters, see fig. 2, had the same probability to be chosen. An even more efficient evolution can be obtained if one gives higher weights to smaller clusters. This is because the relative acceptance of trial cluster moves of type 2, 3 and 4 is approximately 100:10:1.)

(3) The clusters of the selected kind that contain the chosen dimer are searched for. Let $i(c)$ be the number of such clusters and let $i_{max}(c)$ be the upper limit for $i(c)$ (c represents the kind of the cluster: $c = 2, 3, 4$ for a pair, a triplet and a quadruplet, respectively). It is easy to check that at close packing $i_{max}(2) = i_{max}(3) = 2$ and $i_{max}(4) = 4$. These numbers were also found to be maximal in simulations of the DC solid with the following definitions of the clusters:

(i) two dimers form a pair if the distance of their centres of mass is less than 1.2,

(ii) three dimers form a triplet if the distances between their centres of mass are larger than $\sqrt{7}/2$ and less than 1.53,

(iii) four dimers form a quadruplet if the four shorter distances between their centres of mass are within the interval $(\sqrt{7}/2, 1.53)$, whereas the larger

distance of the remaining two distances belongs to the interval (2, 2.31) and the smaller one to the interval $(\sqrt{3}, 2)$.

(4) If the number of the clusters searched for in (3) is positive ($i(c) > 0$) then a random number, $0 \leq \xi < 1$, is generated, and if $\xi < i(c)/i_{max}$, one of these clusters (randomly chosen) is trial replaced by its mirror image with respect to the axis containing the mass centre of the chosen cluster and a centre of one of its atoms (for quadruplets only the four atoms closest to the cluster mass centre are considered). If no overlap is found after this replacement, the move is accepted. Otherwise the previous configuration is not changed.

Two remarks should be added at the end:

(i) as one can check, the cluster moves fulfill the microscopic reversibility condition,

(ii) the acceptance ratio for the cluster moves was found to increase slightly if in place of the real positions of atoms, $\boldsymbol{r}$, rescaled positions, $\boldsymbol{r}'$, were used in the substep (4) according to formula $\boldsymbol{r}' - \boldsymbol{r}_c = \alpha(\boldsymbol{r} - \boldsymbol{r}_c)$, where $\boldsymbol{r}_c$ is the mass centre of the dimer to which the considered atom belongs, and $\alpha \approx \sqrt{v^*}$ is a constant within a single run.

Appendix D. Stability of the DC phase in a free-volume-like lattice model

In this section we consider the lattice model, defined in section 4.2, in which the discs constituting dimers interact via the effective (nearest-neighbour site–site) interaction potential $u(r) = -\frac{2}{3}k_B T \ln(r/\sigma - 1)$. As one can check, a triangular lattice of points interacting via the latter (nearest-neighbour) potential is equivalent to the hard disc system in the self-consistent free volume approximation [34]. Although the self-consistent free volume approximation is known to overestimate the *absolute* free energy of a structure (compare the results of refs. [3] and [34]) we expect that it accurately estimates the free energy *differences* between various crystalline structures. (For example, this approximation predicts the same free energy for the f.c.c. and h.c.p. structures of the 3D hard spheres, what does not contradict the most accurate of the existing estimates [36].) Strictly speaking, in the case of the dimers, the considered lattice model is a certain simplification of the self-consistent free volume approximation. We believe, however, that it preserves the essence of the latter.

As an example of the periodic structure we use the herring-bone lattice B. For the relative area $v^* = 1 + \epsilon$ ($\epsilon \to 0^+$) the equilibrium parameters of this structure can be obtained by minimizing the free energy. In the first-order expansion with respect to ϵ this can be done analytically, and the results are $a \approx 1 + 0.600\epsilon$, $b_x = 0$, $b_y \approx 2\sqrt{3}(1 + 0.400\epsilon)$ and $\phi_{1,2} = \pm\pi/6 \mp 0.346\epsilon$. The

free energy of this structure is equal to

$$f_B(\epsilon)/k_B T \approx -\tfrac{20}{3} \ln \epsilon + 3.406 + \mathcal{O}(\epsilon) . \tag{5}$$

The free energy of the structure A is the same and the free energies of the other periodic structures differ only slightly from this value (less than by $0.1 k_B T$).

The free energy of a typical non-periodic structure can be obtained by considering a random decoration of the kagomé lattice by the dimer centres of mass. The free energy was calculated as an average of the effective interaction between the chosen dimer and neighbouring 'atoms' of other dimers (whose centres of mass were located on the kagomé lattice). To simplify the calculations we neglected any correlations of the positions of the dimers neighbouring to a chosen dimer. The obtained free energy is equal:

$$f^{(\text{typical})}_{\text{non-periodic}}(\epsilon)/k_B T \approx -\tfrac{20}{3} \ln \epsilon + 3.60 + \mathcal{O}(\epsilon) . \tag{6}$$

The free energy of the DC phase is lower than the free energy of the typical non-periodic phase by the degeneracy entropy

$$f_{DC}(\epsilon)/k_B T = -s_{\text{deg}} + f^{(\text{typical})}_{\text{non-periodic}}(\epsilon)/k_B T = -\tfrac{20}{3} \ln \epsilon + 2.74 + \mathcal{O}(\epsilon) . \tag{7}$$

Clearly, at small ϵ the DC phase is more stable than the herring-bone lattice (and the other periodic structures studied).

References

[1] B.J. Alder and T.E. Wainwright, J. Chem. Phys. 27 (1957) 1208; 33 (1960) 1439.
[2] W.W. Wood and J.D. Jacobson, J. Chem. Phys. 27 (1957) 1207.
[3] W.G. Hoover and F.H. Ree, J. Chem. Phys. 49 (1968) 3609.
[4] B.J. Alder and T.E. Wainwright, Phys. Rev. 127 (1962) 359.
[5] J. Vieillard-Baron, J. Chem. Phys. 56 (1972) 4729;
J. Cuesta and D. Frenkel, Phys. Rev. A 42 (1990) 2126.
[6] D. Frenkel and R. Eppenga, Phys. Rev. A 31 (1985) 1776.
[7] R. Eppenga and D. Frenkel, Mol. Phys. 52 (1984) 1303.
[8] D. Frenkel and B. Mulder, Mol. Phys. 55 (1985) 1171.
[9] A. Stroobants, H.N.W. Lekkerkerker and D. Frenkel, Phys. Rev. A 36 (1987) 2929.
[10] D. Frenkel, Liquid Cryst. 5 (1989) 929.
[11] J.A.C. Veerman and D. Frenkel, Phys. Rev. A 41 (1990) 3237.
[12] J.A.C. Veerman and D. Frenkel, Phys. Rev. A 45 (1992) 5632.
[13] A.C. Brańka, P. Pierański and K.W. Wojciechowski, J. Chem. Phys. Solids 43 (1982) 817;
K.W. Wojciechowski, A.C. Brańka and M. Parrinello, Mol. Phys. 53 (1984) 1541.
[14] P. Gerlach, W. Prandl and J. Lefebvre, Mol. Phys. 49 (1983) 991.

[15] S.J. Singer and R. Mumaugh, J. Chem. Phys. 93 (1990) 1278.
[16] A.C. Brańka and K.W. Wojciechowski, Mol. Phys. 72 (1991) 941.
[17] N.D. Mermin, Phys. Rev. A 176 (1968) 250.
[18] S.K. Sinha, ed., Ordering in Two Dimensions (North-Holland, New York, 1980).
[19] C.A. Rogers, Packing and Covering (Cambridge Univ. Press, Cambridge, 1964) p. 81.
[20] (a) R.H. Fowler and G.S. Rushbrooke, Trans. Faraday Soc. 33 (1937) 1272;
(b) J.F. Nagle, Phys. Rev. 152 (1966) 190;
(c) A.J. Phares and F.J. Wunderlich, J. Math. Phys. 27 (1986) 1099.
[21] K.W. Wojciechowski, Phys. Lett. A 122 (1987) 377.
[22] A.C. Brańka and K.W. Wojciechowski, Mol. Phys. 56 (1985) 1419.
[23] A. Bellemans, J. Orbans and D. Van Belle, Mol. Phys. 39 (1980) 781.
[24] J. Talbot and D.J. Tildesley, J. Chem. Phys. 83 (1985) 6419.
[25] K.G. Honnel and C.K. Hall, Mol. Phys. 65 (1988) 1281.
[26] K.W. Wojciechowski, D. Frenkel and A.C. Brańka, Phys. Rev. Lett. 66 (1991) 3168.
[27] K.W. Wojciechowski, J. Chem. Phys. 94 (1991) 4099.
[28] B.J. Alder, W.G. Hoover and D.A. Young, J. Chem. Phys. 49 (1968) 3688.
[29] K.W. Wojciechowski and A.C. Brańka, Phys. Lett. A 134 (1988) 314.
[30] T. Boublik, Mol. Phys. 63 (1988) 685.
[31] D.A. Ward and F. Lado, Mol. Phys. 64 (1988) 1185.
[32] H. Kawamura, Prog. Theor. Phys. 61 (1979) 1584.
[33] J.G. Kirkwood, J. Chem. Phys. 18 (1950) 380.
[34] W.W. Wood, J. Chem. Phys. 20 (1952) 133.
[35] D.A. Young and B.J. Alder, J. Chem. Phys. 60 (1974) 1254.
[36] D. Frenkel and A.J.C. Ladd, J. Chem. Phys. 81 (1984) 3188.
[37] K.W. Wojciechowski, Phys. Rev. B 46 (1992) 26.
[38] J.S. Rowlinson, J. Talbot and D.J. Tildesley, Mol. Phys. 54 (1985) 1065.
[39] M. Widom, K.J. Strandburg and R.H. Swendsen, Phys. Rev. Lett. 58 (1987) 707;
C.L. Henley, J. Phys. A 21 (1988) 1649.
[40] K. Takemura et al., Phys. Rev. B 26 (1982) 998.